

# User's Guide for RAM Versions 1.0 and 1.0p

Michael D. Collins

*Naval Research Laboratory*

*Washington, DC 20375*

## 1 Introduction

The parabolic equation (PE) method [1–4] is very effective for solving range-dependent ocean acoustics problems. This document is a user's guide for the Range-dependent Acoustic Model (RAM), a FORTRAN code based on the latest techniques in PE modeling. Version 1.0 of RAM is designed for single-processor calculations. Version 1.0p can be several times faster than Version 1.0 on a parallel-processing computer. Section 2 describes the PE techniques used in RAM. Section 3 describes the computer code and the format of the input file.

RAM is based on the split-step Padé solution [5,6], which allows large range steps and is the most efficient PE algorithm that has been developed [7]. Range dependence is handled accurately by applying an energy-conservation correction [8,9] as the acoustic parameters vary with range. An initial condition (or starting field) is constructed using the self-starter [10,11], which is an accurate and efficient approach based on the PE method (hence the name).

The numerical solution of the parabolic wave equation involves repeatedly solving tridiagonal systems of equations. This key component of RAM has been optimized by minimizing the number of operations and by using a special elimination scheme that is efficient for problems involving variable ocean depth [12,13]. The split-step Padé algorithm is based on rational function approximations. The tridiagonal systems of equations that correspond to different terms of the rational approximation may be solved in parallel to achieve significant gains in efficiency.

## 2 Parabolic equation techniques

The PE method is based on assuming that outgoing energy dominates back-scattered energy and factoring the operator in the frequency-domain wave equation to obtain an outgoing wave equation. A function of an operator is then approximated using a rational function to obtain an equation that can be solved numerically. By reducing an elliptic boundary-value problem to an initial-value problem in range, run times can be reduced by a factor of several orders of magnitude. This gain in efficiency does not come at the expense of accuracy because range dependence is gradual (so that outgoing energy dominates) in many ocean environments.

We work in cylindrical coordinates, where the range  $r$  is the horizontal distance from a point source,  $z$  is the depth below the ocean surface, and  $\theta$  is the azimuth. Cylindrical spreading is handled by removing the factor  $r^{-1/2}$  from the complex pressure  $p$ . Problems are reduced to two dimensions using the uncoupled-azimuth approximation [14–17], which is valid when horizontal variations in the medium are sufficiently gradual. Range dependence is handled by approximating the medium as a sequence of range-independent regions. An arbitrary level of accuracy may be obtained by using a sufficient number of regions.

Away from the source,  $p$  satisfies the following far-field equation in each range-independent region:

$$\frac{\partial^2 p}{\partial r^2} + \rho \frac{\partial}{\partial z} \left( \frac{1}{\rho} \frac{\partial p}{\partial z} \right) + k^2 p = 0, \quad (1)$$

where  $\rho$  is the density,  $k = (1 + i\eta\beta)\omega/c$  is the wave number,  $\omega$  is the circular frequency,  $c$  is the speed of sound,  $\beta$  is the attenuation in dB/ $\lambda$ , and  $\eta = (40\pi \log_{10} e)^{-1}$ . Factoring the operator in Eq. (1), we obtain

$$\left( \frac{\partial}{\partial r} + ik_0(1 + X)^{1/2} \right) \left( \frac{\partial}{\partial r} - ik_0(1 + X)^{1/2} \right) p = 0, \quad (2)$$

$$X = k_0^{-2} \left( \rho \frac{\partial}{\partial z} \frac{1}{\rho} \frac{\partial}{\partial z} + k^2 - k_0^2 \right), \quad (3)$$

where  $k_0 = \omega/c_0$  and  $c_0$  is a representative phase speed. Assuming that outgoing energy dominates back-scattered energy, we obtain the outgoing

wave equation,

$$\frac{\partial p}{\partial r} = ik_0 (1 + X)^{1/2} p . \quad (4)$$

The formal solution of Eq. (4) is

$$p(r + \Delta r, z) = \exp\left(ik_0\Delta r (1 + X)^{1/2}\right) p(r, z) , \quad (5)$$

where  $\Delta r$  is the range step. Applying an  $n$ -term rational function to approximate the exponential function, we obtain

$$p(r + \Delta r, z) = \exp(ik_0\Delta r) \prod_{j=1}^n \frac{1 + \alpha_{j,n}X}{1 + \beta_{j,n}X} p(r, z) . \quad (6)$$

Version 1.0 of RAM is based on Eq. (6) and is designed for single-processor applications. Expanding the rational function in Eq. (6) by partial fractions, we obtain

$$p(r + \Delta r, z) = \exp(ik_0\Delta r) \left( 1 + \sum_{j=1}^n \frac{\gamma_{j,n}X}{1 + \beta_{j,n}X} \right) p(r, z) . \quad (7)$$

Version 1.0p of RAM is based on Eq. (7) and is useful for parallel processing, with the terms on the right-hand side assigned to different processors. Since the sum form of the rational function is more sensitive to round-off errors than the product form, it is necessary to compile Version 1.0p in double precision when  $k_0\Delta r$  is large.

The complex coefficients  $\alpha_{j,n}$  and  $\beta_{j,n}$  are defined by placing accuracy and stability constraints on the rational function. The accuracy constraints guarantee that the propagating spectrum  $X \cong 0$  is handled accurately. The purpose of the stability constraints, which are essential for the self-starter and the energy-conservation correction, is to annihilate the evanescent spectrum  $\text{Re}(X) < -1$ . RAM computes the coefficients in Eq. (6) by first solving a linear problem for the coefficients of a ratio of two polynomials of degree  $n$  and then using subroutines from [18] to find the roots of the polynomials. The constraints used in RAM are that  $2n - n_s$  derivatives of the rational function are correct at  $X = 0$  and that the rational function vanishes at  $n_s$  points in the evanescent region. We have found that  $n_s = 1$  or  $2$  is effective for most problems. The stability constraints introduce a small amount of artificial attenuation, which is insignificant for most problems but can be

significant for propagation in deep water to very long ranges. To handle this type of problem accurately, RAM provides the option of turning off the stability constraints at a specified range.

The self-starter is an accurate and efficient approach for obtaining an initial condition for Eq. (4). For the case of a line source at  $z = z_0$  in plane geometry, the complex pressure satisfies

$$\frac{\partial^2 p}{\partial x^2} + \rho \frac{\partial}{\partial z} \left( \frac{1}{\rho} \frac{\partial p}{\partial z} \right) + k^2 p = 2i\delta(x)\delta(z - z_0) . \quad (8)$$

Integrating Eq. (8) over an arbitrarily small  $x$  interval about the origin, we obtain

$$\lim_{x \rightarrow 0^+} \frac{\partial p}{\partial x} = i\delta(z - z_0) . \quad (9)$$

Substituting the outgoing wave equation into Eq. (9), we obtain

$$k_0(1 + X)^{1/2} p = \delta(z - z_0) . \quad (10)$$

The initial condition can not be evaluated numerically at  $x = 0$  due to the singularity at the source location. We evaluate the field at  $x = x_0$  to avoid the singularity, where  $x_0$  is on the order of a wavelength. Substituting Eq. (5) into Eq. (10) with  $x_0$  in place of  $\Delta r$ , we obtain

$$p(x_0, z) = \frac{\exp\left(ik_0 x_0(1 + X)^{1/2}\right)}{k_0(1 + X)^{1/2}} \delta(z - z_0) . \quad (11)$$

The self-starter requires a modification for the case of a point source in cylindrical geometry. The normal-mode representation of the acoustic field is used in [10] to show that the self-starter for a point source is of the form,

$$p(r_0, z) = \frac{\exp\left(ik_0 r_0(1 + X)^{1/2}\right)}{k_0^{1/2}(1 + X)^{1/4}} \delta(z - z_0) . \quad (12)$$

To avoid encountering singular intermediate solutions, RAM solves Eq. (12) with the following approach [11]:

$$(1 + X)^2 q(z) = k_0^{-1/2} \delta(z - z_0) , \quad (13)$$

$$p(r_0, z) = (1 + X)^{7/4} \exp\left(ik_0 r_0(1 + X)^{1/2}\right) q(z) . \quad (14)$$

The intermediate function  $q$  has two continuous derivatives. A rational-linear function is used to approximate the operator in Eq. (14).

The solution is advanced through each of the range-independent regions using Eq. (6) or (7). For range-dependent problems, it is necessary to specify a condition at the vertical interfaces between regions. Accurate solutions may be obtained by conserving the energy flux,

$$E = \text{Im} \int \rho^{-1} p^* \frac{\partial p}{\partial r} dz . \quad (15)$$

The normal-mode representation is used in [19] to show that energy flux may be conserved by conserving the linear quantity,

$$A = \rho^{-1/2} k_0^{1/2} (1 + X)^{1/4} p . \quad (16)$$

In the limit of nearly horizontal propagation,

$$A \sim p/\alpha , \quad (17)$$

where  $\alpha = (\rho/k)^{1/2}$ . Conserving  $p/\alpha$  provides accurate solutions for most problems in ocean acoustics. To conserve energy, RAM is implemented using the modified dependent variable  $\tilde{p} = p/\alpha$  and the modified depth operator,

$$\tilde{X} = k_0^{-2} \left( \frac{\rho}{\alpha} \frac{\partial}{\partial z} \frac{1}{\rho} \frac{\partial}{\partial z} \alpha + k^2 - k_0^2 \right) . \quad (18)$$

Since different quantities are conserved across horizontal ( $p$ ) and vertical ( $p/\alpha$ ) interfaces, Gibbs oscillations can occur for problems involving sloping interfaces. The stability constraints annihilate these artifacts, which project onto the evanescent spectrum.

The depth operator  $\tilde{X}$  is discretized using Galerkin's method as described in [9]. This approach for replacing the depth operator with a tridiagonal matrix handles piece-wise continuous depth variations in the acoustic parameters. After discretizing in depth, the numerical solution involves repeatedly solving tridiagonal systems of equations. As Figure 1 indicates, Gaussian elimination involves sweeping downward to eliminate entries below the main diagonal followed by back substitution sweeping upward. The entries near the ocean bottom interface change when bathymetry varies, and it is necessary to repeat the downward elimination throughout the ocean bottom. The

other elimination scheme illustrated in Figure 1 is more efficient for problems involving variable ocean depth. Elimination begins at both the top (entries below the main diagonal are eliminated) and bottom (entries above the main diagonal are eliminated) of the grid and ends at the ocean bottom interface. Back substitution then proceeds in both directions from the ocean bottom. With this approach, it is necessary to modify only a few rows of the matrices when ocean depth varies.

### 3 Computer implementation

In this section, we discuss how to run RAM and how the code is organized. Since `ram.f` (Version 1.0) and `ramp.f` (Version 1.0p) are relatively short and simple codes, they are easy to modify for special applications such as interfacing with a data base, outputting data in a particular format, or using as a subroutine for another code. The files in the RAM package include `ram.f`, `ramp.f`, `ram.in`, `ram.jpg`, and `ram.ps`. These files are available via anonymous ftp from `ram.nrl.navy.mil` in the directory `/ftp/pub/ram`.

The main part of `ram.f` contains a call to the subroutine `setup` to initialize parameters, a loop that marches the solution in range, a call to `outpt` to write out transmission loss, and a call to `updat` to update the tridiagonal matrices when the environment varies with range. Subroutine `setup` reads in and defines parameters, initializes the profiles and tridiagonal matrices, and constructs the starting field. Subroutines `profl` and `zread` read in the profiles and interpolate them onto the grid and define the functions that appear in Eq. (18) in the water column and in the bottom. Subroutine `matrc` sets up the tridiagonal matrices and the special decomposition described in Section 2. Subroutine `solve` solves the tridiagonal system using the decomposed matrices. Subroutine `outpt` writes out transmission loss at  $z = z_r$  at every range to `t1.line` and on a decimated range-depth grid to `t1.grid`. Subroutine `updat` modifies the matrices when ocean depth varies (this procedure requires little effort) and reconstructs the matrices when the profiles are updated.

Subroutine `epade` computes the coefficients of the rational function with the help of several other subroutines including subroutines from [18] for finding the roots of a polynomial. Subroutine `epade` writes out to `pade.check` the values of the rational functions and the functions they approximate over

a set of points that includes both the propagating and evanescent spectrum. This file can be used to determine appropriate values for  $n$  and  $c_0$ . The subroutines that compute the coefficients of the rational approximation are written in double precision. Everything else is written in single precision. For some computers and applications, it is necessary to modify the precision for the codes or parts of the codes. Double precision is required for `ramp.f` when  $k_0\Delta r$  is large. Double precision is required for both `ram.f` and `ramp.f` when the number of depth grid points is large.

The form of the input file `ram.in` is illustrated in Figure 2. Many of the inputs that are defined in Figure 3 correspond to parameters defined in Section 2 and are self-explanatory. The first line of `ram.in` contains the `title`, which may be any string of characters. The decimation factors `ndr` and `ndz` are the number of range and depth grid spacings between output to `t1.grid`. The maximum depth of output to `t1.grid` is `zmlt`. The depth of the ocean is defined by the bathymetry points `rb` and `zb`, with linear interpolation between the input points. The stability constraints are turned off at the range `rs`. This option can be used for long-range propagation in deep water to prevent the introduction of artificial attenuation. When `rs` is set to `0`, the stability constraints are used for all ranges.

The profile block(s) follow the bathymetry block. The range of the profile block `rp` must be specified for each profile block after the first one. Since there is no limit to the number of profile blocks, RAM can handle complex environments. The sample input file appearing in Figure 2 has two profile blocks. The speed of sound in the water column  $c_w$  and the bottom  $c_b$  are constructed from `cw` and `cb`. The density  $\rho_b$  and attenuation  $\beta_b$  in the bottom are constructed from `rhob` and `attn`. In the water column, the density is assigned the value  $\rho_w = 1$  g/cc and the attenuation is assumed to vanish. To prevent artificial reflections, the bottom of the computational grid (the depth `zmax`) is placed well below the ocean bottom interface and the attenuation is increased over the lower few wavelengths of the grid. The profiles are linearly interpolated in depth between the input values and are assumed constant (not extrapolated) outside the range of input. With this convention, the number of inputs is minimized (e.g., constant profiles are defined in the sample input file simply by specifying the value at  $z = 0$ ).

For problems involving variable ocean depth  $d(r)$ , the acoustic parame-

ters are defined as follows:

$$c(r, z) = \begin{cases} c_w(z) & \text{for } z < d(r) \\ c_b(z) & \text{for } z > d(r) \end{cases} \quad (19)$$

$$\rho(r, z) = \begin{cases} \rho_w & \text{for } z < d(r) \\ \rho_b(z) & \text{for } z > d(r) \end{cases} \quad (20)$$

$$\beta(r, z) = \begin{cases} 0 & \text{for } z < d(r) \\ \beta_b(z) & \text{for } z > d(r) \end{cases} \quad (21)$$

The profiles are not interpolated in range. Range dependence in  $c_w$ ,  $c_b$ ,  $\rho_b$ , and  $\beta_b$  is handled by updating `cw`, `cb`, `rhob`, and `attn` abruptly at the range `rp`. If gradual range dependence is desired, it is necessary to either use an appropriate sequence of profile blocks or modify `ram.f` to interpolate profiles.

The problem defined in Figure 2 involves range-dependent sound speed and bathymetry. There is a surface duct in the upper part of the water column for  $r < 25$  km. The sound speed in the water column is homogeneous for  $r > 25$  km. There is an absorbing layer in the lower 100 m of the ocean bottom. A relatively large value is used for  $c_0$  in order to obtain an accurate rational approximation for phase speeds between 1500 and 1700 m/s. The RAM solution appearing in Figure 4 for this problem is accurate for a range step of 500 m. To achieve similar accuracy with finite-difference algorithms that predate the split-step Padé algorithm [20–22], it is necessary to use a range step of about 5 m. For this problem, the split-step Padé solution therefore provides an efficiency gain of about an order of magnitude with a single processor and about two orders of magnitude with parallel processing. A color image of the solution of this problem appears in the file `ram.jpg`.

RAM provides accurate solutions for ocean acoustics problems provided the inputs are selected properly. Accuracy may be controlled by performing simple convergence tests to determine an appropriate parametrization of the environment and appropriate values for the grid spacings, the number of terms in the rational approximation, the value of the reference sound speed, the location of the lower boundary, and the thickness of the absorbing layer. The size of  $\Delta r$  is limited by the rate of range dependence. When range dependence is strong (i.e., the ocean bottom interface is relatively steep), it is necessary to use a relatively large number of range-independent regions. The size of the smallest region is an upper bound on  $\Delta r$ . When the rate



of range dependence varies significantly, efficiency can be improved by modifying `ram.f` to allow a variable range step. The transmission loss data in `tl.line` is useful for convergence tests.

## 4 Acknowledgments

This work was supported by the Office of Naval Research. The author thanks R. J. Cederberg for helping develop efficient techniques for obtaining rational-linear approximations and A. B. Baggeroer for pointing out the need to turn off the stability constraints for some problems.

## References

- [1] M. A. Leontovich and V. A. Fock, “Solution of the problem of propagation of electromagnetic waves along the earth’s surface by the method of parabolic equation,” *J. Exp. Theor. Phys.* **16**, 557–573 (1946).
- [2] V. A. Fock, *Electromagnetic Diffraction and Propagation Problems* (Pergamon, New York, 1965), pp. 213–234.
- [3] F. D. Tappert, “The parabolic approximation method,” in *Wave Propagation and Underwater Acoustics*, edited by J. B. Keller and J. S. Papadakis, Lecture Notes in Physics, Vol. 70 (Springer, New York, 1977).
- [4] F. B. Jensen, W. A. Kuperman, M. B. Porter, and H. Schmidt, *Computational Ocean Acoustics* (American Institute of Physics, New York, 1994), pp. 343–412.
- [5] M. D. Collins, “A split-step Padé solution for parabolic equation method,” *J. Acoust. Soc. Am.* **93**, 1736–1742 (1993).
- [6] M. D. Collins, “Generalization of the split-step Padé solution,” *J. Acoust. Soc. Am.* **96**, 382–385 (1993).
- [7] M. D. Collins, R. J. Cederberg, D. B. King, and S. A. Chin-Bing, “Comparison of algorithms for solving parabolic wave equations,” *J. Acoust. Soc. Am.* (submitted, August 1995).
- [8] M. B. Porter, F. B. Jensen, and C. M. Ferla, “The problem of energy conservation in one-way models,” *J. Acoust. Soc. Am.* **89**, 1058–1067 (1991).

- [9] M. D. Collins and E. K. Westwood, “A higher-order energy-conserving parabolic equation for range-dependent ocean depth, sound speed, and density,” *J. Acoust. Soc. Am.* **89**, 1068–1075 (1991).
- [10] M. D. Collins, “A self-starter for the parabolic equation method,” *J. Acoust. Soc. Am.* **92**, 2069–2074 (1992).
- [11] R. J. Cederberg and M. D. Collins, “An efficient forward model and experimental configuration for geoacoustic inversion,” *J. Acoust. Soc. Am.* (submitted, May 1995).
- [12] M. D. Collins, “Benchmark calculations for higher-order parabolic equations,” *J. Acoust. Soc. Am.* **87**, 1535–1538 (1990).
- [13] G. Strang, *Introduction to Linear Algebra* (Wellesley-Cambridge, Wellesley, 1993), p. 87.
- [14] J. S. Perkins and R. N. Baer, “An approximation to the three dimensional parabolic-equation method for acoustic propagation,” *J. Acoust. Soc. Am.* **72**, 515–522 (1982).
- [15] M. D. Collins and S. A. Chin-Bing, “A three-dimensional parabolic equation model that includes the effects of rough boundaries,” *J. Acoust. Soc. Am.* **87**, 1104–1109 (1990).
- [16] D. Lee, G. Botseas, and W. L. Siegmann, “Examination of three dimensional effects using a propagation model with azimuth-coupling capability (FOR3D),” *J. Acoust. Soc. Am.* **91**, 3192–3202 (1992).
- [17] M. D. Collins, B. E. McDonald, K. D. Heaney, and W. A. Kuperman, “Three-dimensional effects in global acoustics,” *J. Acoust. Soc. Am.* **97**, 1567–1575 (1995).
- [18] F. H. Press, S. A. Teukolsky, W. T. Vetterling, and B. P. Flannery, *Numerical Recipes in FORTRAN* (Cambridge University Press, Cambridge, 1992), Second Edition, pp. 362–368.
- [19] M. D. Collins, “An energy-conserving parabolic equation for elastic media,” *J. Acoust. Soc. Am.* **94**, 975–982 (1993).
- [20] D. Lee, G. Botseas, and J. S. Papadakis, “Finite-difference solution to the parabolic wave equation,” *J. Acoust. Soc. Am.* **70**, 795–800 (1981).
- [21] M. D. Collins, “Applications and time-domain solution of higher-order parabolic equations in underwater acoustics,” *J. Acoust. Soc. Am.* **86**, 1097–1102 (1989).
- [22] F. B. Jensen and C. M. Ferla, “Numerical solutions of range-dependent benchmark problems,” *J. Acoust. Soc. Am.* **87**, 1499–1510 (1990).

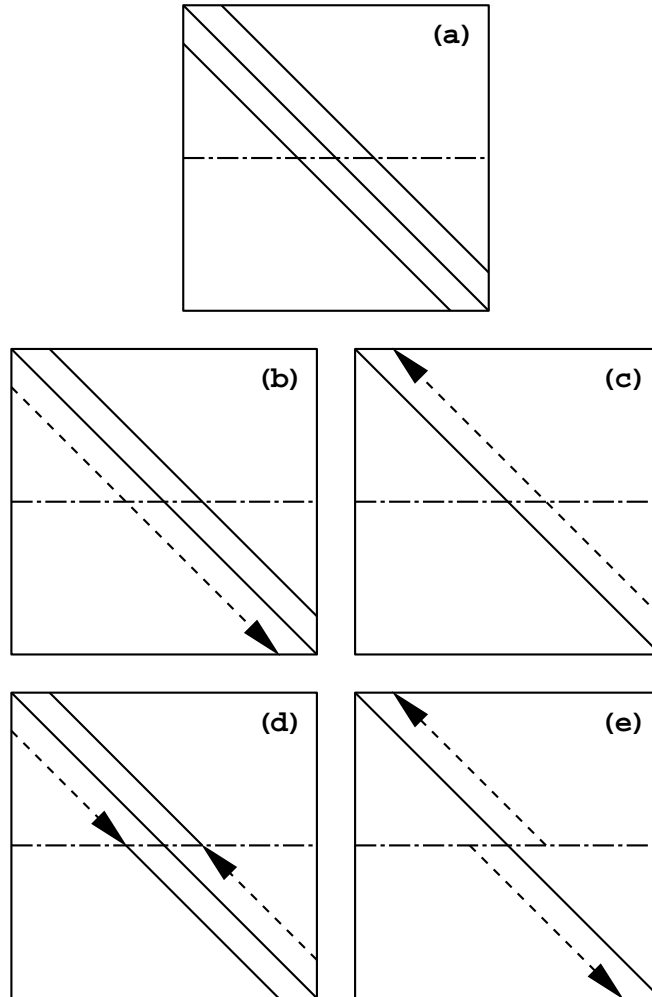


Figure 1: Techniques for solving tridiagonal systems. (a) The matrix prior to elimination. The solid lines indicate the three diagonals. The broken line corresponds to the ocean bottom interface. The dashed lines indicate: the (b) elimination and (c) back substitution steps of Gaussian elimination; the (d) elimination and (e) back substitution steps of a scheme designed to efficiently handle varying bathymetry.

```

range-dependent example  title
50.0 50.0 50.0          freq zs zr
50000.0 500.0 1        rmax dr ndr
1000.0 2.0 1 500.0    zmax dz ndz zmplt
1600.0 8 1 0.0        c0 np ns rs
0.0 200.0              rb zb
40000.0 400.0
-1 -1
0.0 1480.0             z cw
100.0 1520.0
400.0 1530.0
-1 -1
0.0 1700.0            z cb
-1 -1
0.0 1.5               z rhob
-1 -1
900.0 0.5             z attn
1000.0 10.0
-1 -1
25000.0               rp
0.0 1530.0            z cw
-1 -1
0.0 1700.0            z cb
-1 -1
0.0 1.5               z rhob
-1 -1
900.0 0.5             z attn
1000.0 10.0
-1 -1

```

Figure 2: Sample input file `ram.in`. Lines with `-1 -1` are used to indicate the end of the bathymetry and profile blocks.

title	arbitrary string of characters
freq	source frequency (Hz)
zs	source depth (m)
zr	receiver depth for tl.line (m)
rmax	maximum range (m)
dr	range step (m)
ndr	range decimation factor for tl.grid (1=no decimation)
zmax	maximum depth (m)
dz	depth grid spacing (m)
ndz	depth decimation factor for tl.grid (1=no decimation)
zmplt	maximum depth of output to tl.grid
c0	reference sound speed (m/s)
np	number of terms in rational approximation
ns	number of stability constraints (1 or 2)
rs	maximum range of stability constraints (m)
rb	range of bathymetry point (m)
zb	depth of bathymetry point (m)
z	depth of profile point (m)
cw	sound speed in water column (m/s)
cb	sound speed in sediment (m/s)
rhob	density in sediment (g/cc)
attn	attenuation in sediment (dB/wavelength)
rp	range of profile update (m)

Figure 3: Definition of the parameters that appear in ram.in.

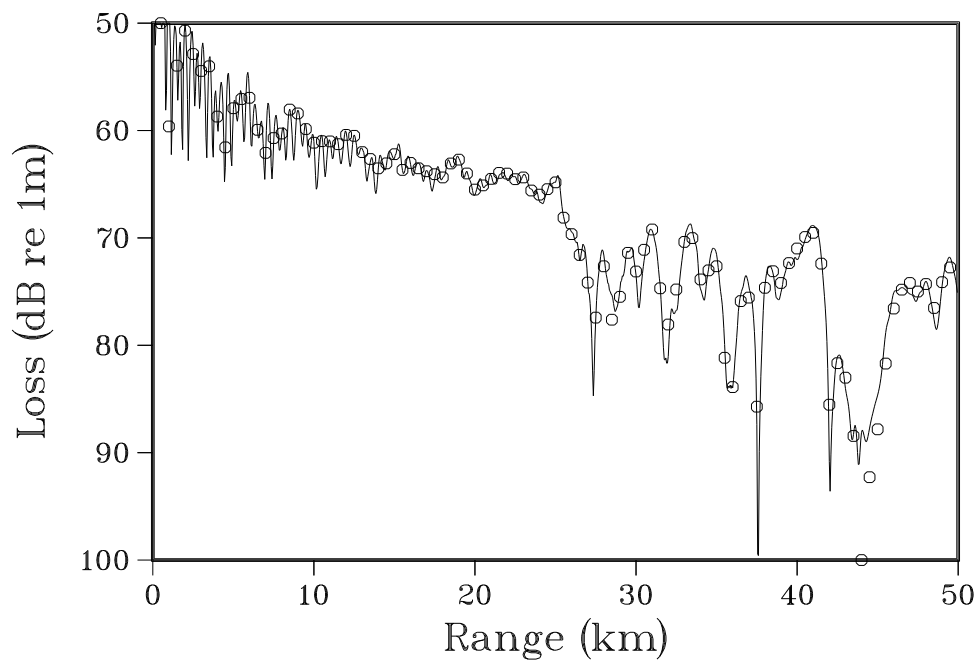


Figure 4: Transmission loss at  $z = 50$  m for the test problem defined in Figure 2. The reference solution is given by the solid curve. The RAM solution is represented by the circles that are spaced by 500 m in range.